Available online at www.asric.org
ASRIC Journal on Engineering Sciences Vol.3(2)(2023) 146-156

Maximum Power Point Tracking and Performance Improvements of Photovoltaic Generator Powered DC Motor pump System based on Fuzzy Logic Controller

Gebrehiwot Fisseha Teklay[1*], Kebede Esayas Kassa[2]

[1]Mekelle University, Ethiopia
[2]Ethiopian Telecominication(Ethiotelecom)

*Corresponding auth]or: Gebrehiwot Fisseha Teklay

Abstract
The maximum extractable power of diode junction photovoltaic generators exhibits a nonlinear V-I characteristic that varies with solar radiation intensity, temperature, and load conditions. In PV generator applications, a maximum power point tracking (MPPT) controller was used to automatically extract the maximum power, regardless of the PV system's actual instantaneous conditions. The P&O and the incremental conductance, out of the various MPPT approaches previously proposed, have an advantage in low-cost implementation, but their drawback is having high oscillations. In this thesis, a fuzzy logic control (FLC) method is presented for maximizing the output of a standalone PV generator for a water pumping system. A solar panel, a DC-DC buck converter, a fuzzy MPP tracker, a permanent DC motor drive, and a centrifugal pump make up the PV generator system. The coupled centrifugal pump's motor speed and water discharge rate maximized because of the duty ratio of the buck chopper being adjusted by the fuzzy logic controller to meet the load impedance of the photovoltaic generator. The control approach has been modeled in MATLAB/SIMULINK, and simulation results have indicated that, when compared to a directly connected PV-generator-energized pumping system, it has greatly enhanced the system's power extraction performance under various sunshine situations.
Keywords: Centrifugal pump, Diode junction photovoltaic, DC-DC buck converter, DC motor, FLC, MPPT

1. Introduction
Water is essential for life and for most activities in human society. Most human activities and needs rely upon excess water supplies, such as ensuring food production and protecting health, energy, and the restoration of ecosystems. All societies require water for social, economic, and sustainable development (UNEP, 2015). There is an urgent need to supply sustainable energy for the provision of drinking water at very low financial and environmental costs, especially in relatively arid and rural regions. Without basic services, such regions are likely to become aid-dependent or depopulated and unproductive, especially when expectations are raised by modern information and communications technology. Remote PV water pumping and PV power generation systems generally seem to be excellent solutions to address this problem in the future.

In rural areas, pumping systems are required to pump water for domestic use, irrigate crops, and water cattle and animal stocks. Hence, a power source was required to operate the pumping system. An AC-powered system is economical and requires minimal maintenance when AC power is available from the nearby grid. However, in many rural areas, water sources are spread over many miles of land and are located too far from existing grid lines. The installation of a new transmission line and transformers at isolated locations is extremely expensive. Photovoltaic energy has gained considerable attention in recent years because it is environmentally friendly and sustainable compared to traditional energy sources. .In this study, the fuzzy logic MPPT controller is applied and evaluated using a minimal complexity, robust system comprising a DC motor pump drive. The system was simulated and analyzed using MATLAB/Simulink, and the energy utilization efficiency was calculated for different levels of irradiation and temperature.

We propose a stand-alone water-pumping system in this thesis. This will be utilized in conjunction with a water storage tank rather than battery storage to meet the needs of an isolated, remote, low-maintenance, and low-cost water-pumping application. As shown in Figure 1, the system consists primarily of a solar array as a source, which converts sunlight into electrical energy, and a centrifugal pumping load driven by a permanent magnet DC motor. A maximum power point tracker is required to achieve high-efficiency system performance and improve the quantity of energy taken from the PV array by the load during daylight hours.

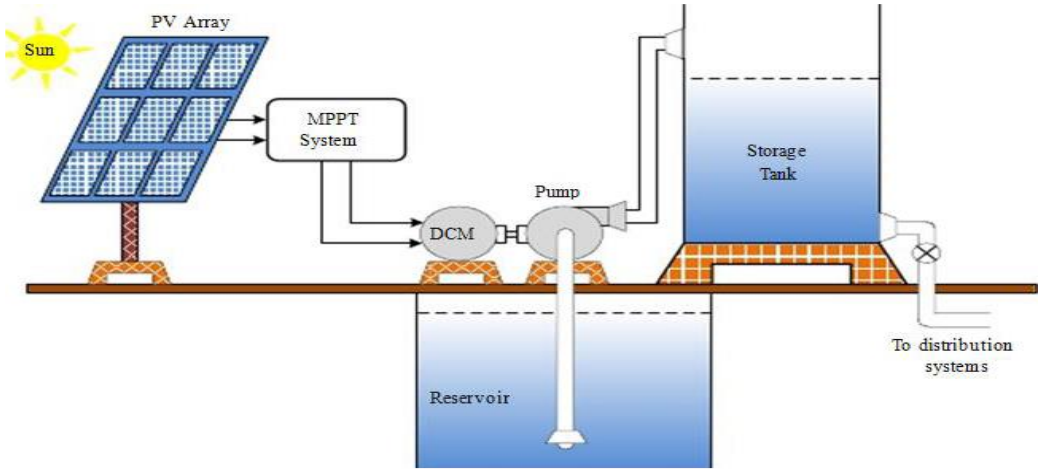

Figure 1. Block diagram of standalone PV water pumping system (Muta T, et al.1995)

2. Methods and Materials

Modelling and Design of Standalone PV Water Pumping System

Wajirat is a town in Ethiopia's Tigray region. It is located about 67 kilometers south of Mekelle in the Tigray zone. The town has an elevation of 2200 meters above sea level and an altitude and longitude of 13°15N39°31E, respectively. It is one of the most populous communities in the Hintalo Wajirat district. According to central statistical agency Ethiopia, figures from 2005, this town had an estimated total population of 30,900 in 1997, and the E.C. census showed a total population of 50,762. The purpose of this thesis was to tackle the water difficulties of 60000 residential houses in Wajirat Debub Wereda.

It will be determined using the following input data if there are 6,000 residential homes and an average of four persons in a family to satisfy the minimal water needs of the population from ground water: The appropriate pump will be determined by the above data if the selected well depth is 150 m, the drawdown is 20 m, and the safe yield in that location is 19 L/s.

Table 1: Minimum water requirement assumptions in a day per person in a family

Activities	Drinking	Cooking	Personal washing	Cleaning home	Average no of family members	Total
Water used L/day	3	3 3	10 10	5 5	44 84	84

Then total water need $(Qday) = (No\ of\ residential\ houses) \times (their\ needs\ of\ water)$
$= 6{,}000 \times 84 = 504{,}000 L/day$

The total lifting height (T_h) is the major parameter utilized in a solar pumping system to determine the required power to transport the water from the well depth level to the required location. (N. Hajj Shehadeh, 2015)

$$T_h = P_h + V_{Rh} + f_h + V_h + D_h + H_{pipe} \quad (1)$$

Where, V_{Rh} = vertical rise head, P_h= pump level head, f_h =A head due to friction loss, V_h =velocity head, D_h=Dynamic head loss, T_h =Total system dynamic head, H_{pipe}=horizontal length of the pipe.

To calculate f_h apply Darcy -Weisbach formula. (N. Hajj Shehadeh, 2015)

$$f_h = \frac{4f \times L \times c}{dg} \quad (2)$$

Where, *f*=friction factor, *L*=length of pipe, *d*=pipe diameter and *c*=mean velocity fluid and *f* is more problematic for smooth flow and smooth pipes. Blasius equation is applicable (N. Hajj Shehadeh, 2015).

$$f = \frac{0.079}{R_e^{1.4}} \quad (3)$$

It can simplified to $f = \frac{64}{R_e}$, if Reynolds number is greater than 400 $\left(\boldsymbol{R_e} = \frac{\boldsymbol{\rho \times v \times d}}{\boldsymbol{\mu}} \right)$

The amount of power required to take the ground water surface (N. Hajj Shehadeh, et al., 2015)

$$E = m \times g \times (Th)\eta = \rho V g(T_h)\eta \quad (4)$$

$$since\ m = \rho V$$

Where, *m*=the mass of the water needed (kg), *g*=the acceleration due to gravity (m/s2), *Th*= Total system head (m), *η*= Efficiency of the system, *E*=Energy required to move the water from level to head, *V*= volume of the tanker inm^3.

The pump should provide the required flow rate and transfer water into the system's total dynamic head to fill the required number of liters. That is to raise 504 m^3 of water at a head of 96.78m and a flow rate of 43 m^3/h using the typical 17.18 KW motor.

A p-n junction diode coupled in parallel with the current source is commonly used to illustrate the basic solar cell. The photocurrent produced by sunlight is represented by the current source, and the current-voltage characteristic of the cell is determined by the diode.

$$I_{pv} = I_{ph} - I_D \quad (5)$$

The internal diffusion current,I_D, and the light-generated current, I_s , are proportional to the radiation and surface temperature. The output current and voltage of the solar cell is represented by I_{PV} andV_{PV}, respectively. The diode internal diffusion current is modeled by (Villalva, et al., 2009).

$$ID = I_S.[exp(q.V_{pv}A.K.T_c) - 1] \quad (6)$$

The photocurrent is connected to the cell's operating temperature and solar intensity as shown (7)

$$I_{ph} = \left[I_{SC} + K_I \times \left(T_C - T_{Ref}\right)\right] \times \frac{G}{G_{ref}} \quad (7)$$

Where, I_{SC} is the short-circuit current is known from the data sheet K_I is the temperature coefficient of the cell's short circuit current (amperes/ K), T_{Ref} is the cell reference temperature in Kelvin, $T_{Ref} = 298\,k\ (250C)$, G is the solar isolation in W/m2 and Gr represents the reference solar radiation W/m2, Gr = 1kW/m2. Short circuit is measured under the standard test condition at a reference temperature of 250C and solar radiation$1kW/m^2$. The general model shown in Figure 2 is accurate, because it includes the parasitic elements, shunt resistance Rsh and series resistant Rs.

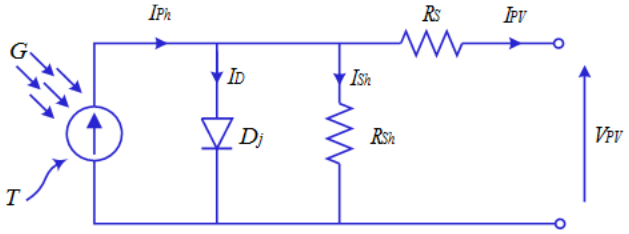

Figure 2: complete general model of photovoltaic cell (Villalva, et al. 2009).

The PV cell output currentI_{PV}, expressed:

$$I_{pv} = I_{ph} - I_s.\left[e^{\frac{q.(V_{pv}+I_{pv}R_S)}{A.K.T_C}} - 1\right] - \left(\frac{V_{pv}+I_{pv}.R_s}{R_{sh}}\right) \quad (8)$$

The PV efficiency is unaffected by the variable,R_{sh} which can be considered to approach infinity in the absence of leakage current. As a result, the R_{sh} can be ignored to produce the appropriate model with the appropriate difficulty.

$$I_{pv} = I_{ph} - I_s.\left[e^{\frac{q.(V_{pv}+I_{pv}R_S)}{A.K.T_C}} - 1\right] \quad (9)$$

Table 2: The proposed module and array values (Aashoor, et al. 2012)

Electrical Characteristics of Sun power E19 /240W @1000W/m² 1.5AM 25°C		
The PV parameters	Module value	Array value
Rated power(p_{max})	240W	29040W
Maximum Power Voltage (V_{pm})	40.5V	445.5V
Maximum Power Current (I_{pm})	5.93A	65.23A
Open-Circuit Voltage (V_{oc})	48.6V	534.6V
Short-Circuit Current (I_{sc})	6.3A	69.3A
Temperature Coefficient (P_{max})	-0.38%/° C	-0.38%/° C
Temperature Coefficient (V_{oc})	-132.5mV/° C	-132.5mV/° C
Temperature Coefficient (I_{sc})	3.5mA/° C	3.5mA/° C
Cell Efficiency (η_{cell})	20 %	20 %
Numbers of cells (Ns)	96	11616
Module Efficiency (η_{mod})	19.3%	19.3%
Series Resistance (R_s)	0.2746Ω	0.2746Ω
Energy band gap (E_{gap})	1.12 for silicon	-
Diode ideality factor (A)	1	-

When a fixed resistive load (R) is directly connected to the PV cell's terminal, the operating point is determined by the junction of the solar cell's I-V characteristic and the load's I-V characteristic.

Mathematical Modeling for Dc Motor And Pump

Many research have been conducted on the use of DC motors in PV pumping systems rather than AC motors, with the conclusion that DC motors might be directly linked to the PV array. This considerably reduces the overall system cost and complexity. When compared to other PV electro-mechanical systems, the permanent magnet DC motor (PMDCM) combined with a centrifugal pump has suitable matching characteristics with the PV array features and has a low starting torque.

$$P_{peak} = \left(\frac{(B_m\omega_m + T_L)}{K_t}\right)^2 R_a + B_m\omega_m^2 + T_l\omega_m^2 \quad (10)$$

$$P_{peak} = \frac{R_a^2}{K_t}(B_m^2\omega_m^2 + 2B_m\,\omega_m\,T_L + T_L^2\,) + B_m\omega_m^2 + T_L\,\omega_m \quad (11)$$

Since the load is constant, the equation is rearranged to:

$$\left(\frac{B_m^2\,R_a}{K_t^2} + B_m\right)\omega_m^2 + (2B_m\,T_L\,R_aK_t^2 + T_L\,)\omega_m + T_L^2\,R_aK_t^2\, - P_{peak} = 0 \quad (12)$$

In PV pumping systems, both volumetric and centrifugal pumps are commonly employed. Because a DC motor driving a constant volume pump requires a nearly constant current, a load composed of a DC motor driving a constant volume pump is a non-matched load for a PV array. However, it was discovered that in the PV array, the energy utilized by the centrifugal pump works for longer periods of time even at low insulation levels, and its load characteristic is well matched to the PV array's maximum power locus (Anis, W. R., & Metwally, H. M,1994).

The speed-torque characteristics of centrifugal pump including friction torque are approximately given.

$$T_p = T_L = A_L\,K_L\omega_m^{1.8} \quad (13)$$

By substituting (12) into (13) yields,

$$\left(\frac{K_L^2R_a}{K_t^2}\right)\omega_m^{3.6} + (2B_mK_LR_aK_t^2 + K_L)\omega_m^{2.8} + \left(\frac{B_m^2R_a}{K_t^2} + B_m\right)\omega_m^2 - P_{peak}\, = 0 \quad (14)$$

Fuzzy Logic Controller Based MPPT of PV Water Pumping

The variation of solar radiation is the most critical component in a PV system's MMPT. It varies in a nonlinear and periodic manner; thus, an FLC-based MPPT is proposed to solve the problem and transfer the maximum available power of the PV array to the load. A PV array, a buck converter, a fuzzy-based MPPT control unit, and a DC permanent magnet motor linked to a centrifugal pump compose the system. A buck converter transfers

the electricity generated by the PV array to the DC motor. The change in PV array output power and the change in pump rotation speed, are employed as input variables of the fuzzy control unit to determine the duty-ratio control signal (Dadios, E. ed., 2012).

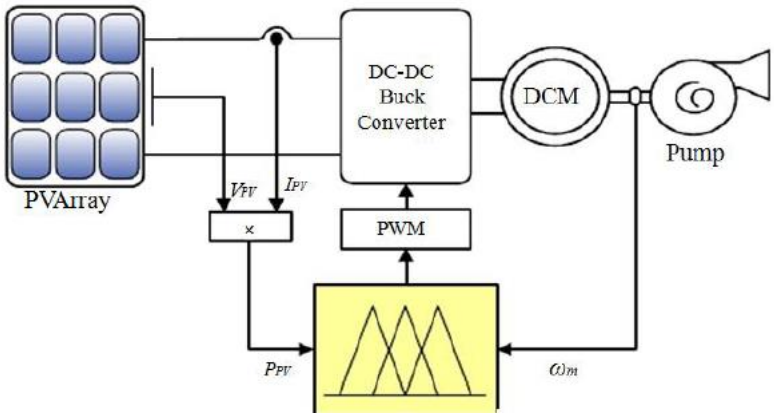

Figure 3: Schematic diagram of MPPT water pumping system based FLC (Dadios, E. ed., 2012).

The control goal is to track the maximum power point and keep the system running at all temperatures and solar irradiation levels, maximizing the DC motor speed and water discharge rate of the associated centrifugal pump. The hydraulic power,$P_p = KT\omega_m^3$, is highest when the PV array's output power is high. As a result, at the highest power point, the rotational speed is at its maximum. A fuzzy logic controller has been proposed to adjust the buck converter duty ratio, which adapts the PV array output power to maximize the rotational speed, which in turn increases the water discharge of the centrifugal water pump, by making use of the relationship between the PV array output power and the rotational speed.

3. Results and Discussion

The entire simulation model of the system is made up of masked blocks that are linked together. The simulation was carried out by connecting a PV model to a PMDCM generating a centrifugal pump load via a regulated buck chopper. An MPPT control device is also incorporated, to validate the performance of the suggested fuzzy logic control technology, a comparison was done between a directly linked system and the proposed method at various ambient temperatures and sunlight insolation levels.

As already stated, the fuzzy logic controller is modeled in MATLAB/SIMULIIK and implemented in the simulation depicted in Figure 4. As shown in Figure 5, the solar irradiation was quickly shifted up and down to test the performance and demonstrate the significant improvement in power extraction of the system employing

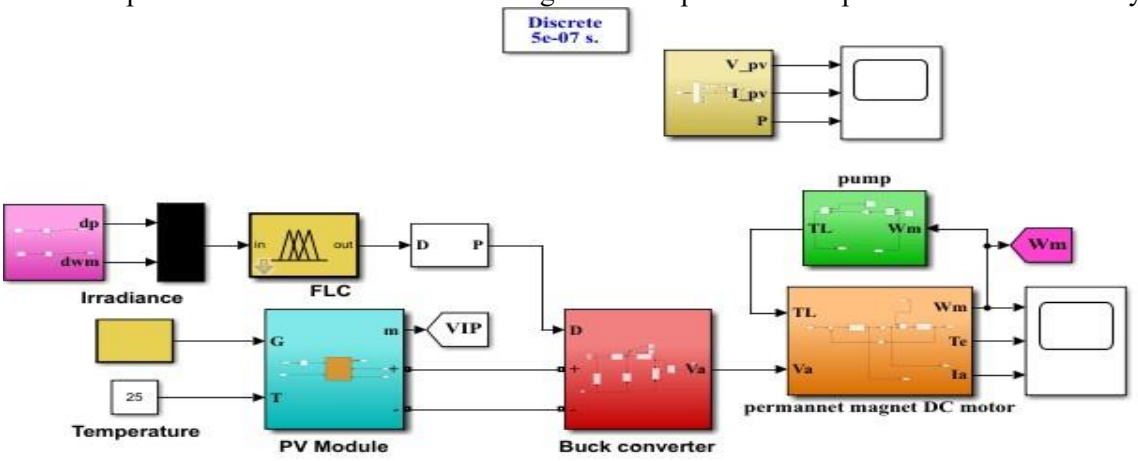

the FLC MPPT compared to the directly connected system. Figures 6 to 16 show simulation results for PV current, voltage, and power, armature voltage and current, load and motor torque, duty cycle, and motor rotational speed, respectively.

Figure 4: SIMULINK model of PV water pumping system with fuzzy MPPT controller

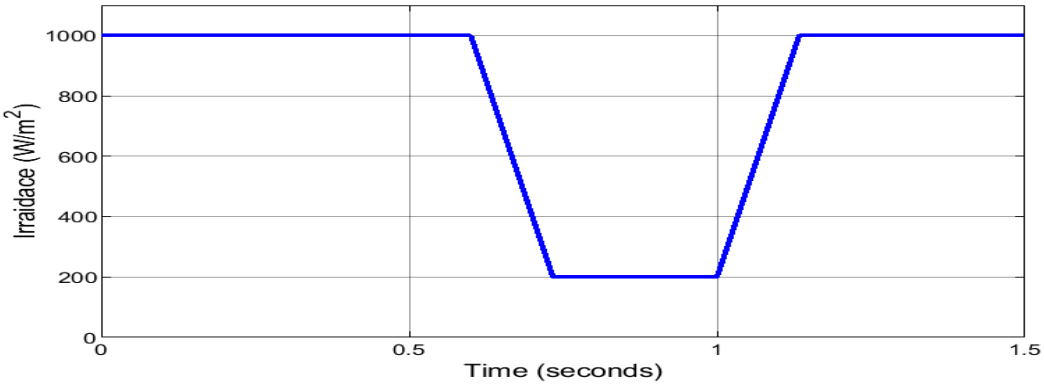

Figure 5: Solar Irradiation

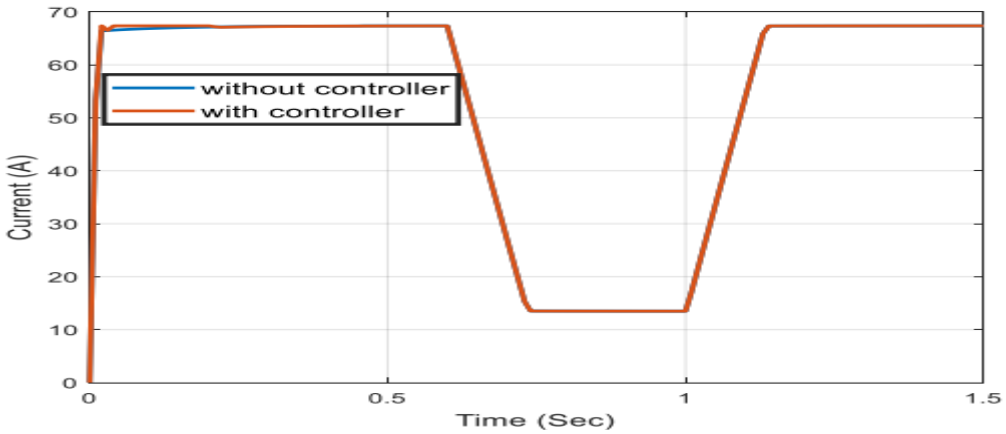

Figure 6: PV array output current for FLC MPPT controller

With the FLC controller connected, the simulation indicates that the system operates near the maximum power point at all irradiation levels. The PV array current is more than the ideal current, as shown in figure. When using a controller, the current increases, but just slightly when compared to the voltage increase.

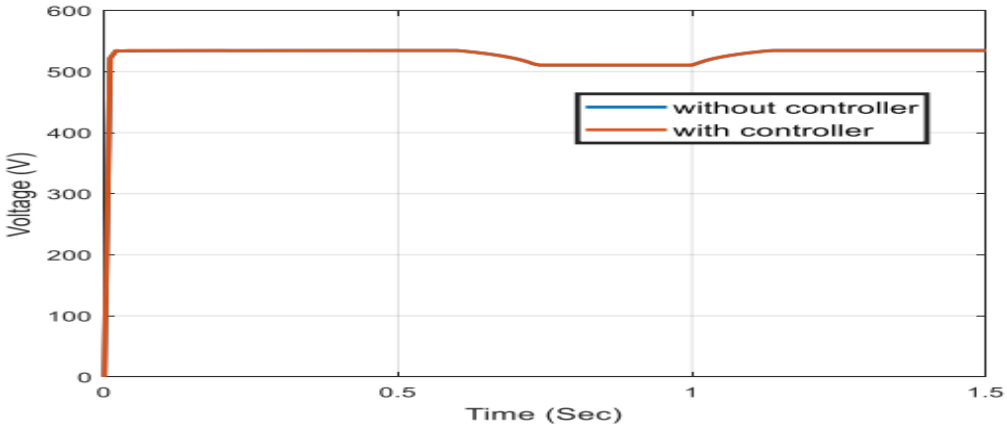

Figure 7: PV array output voltage for MPPT controller

The simulation shows that the directly connected system operating voltage of the PV array voltage is approximately less to the optimal voltage. As a result of this, the system deviates from the maximum operating power all the time. But with FLC controller the operating power is near to the

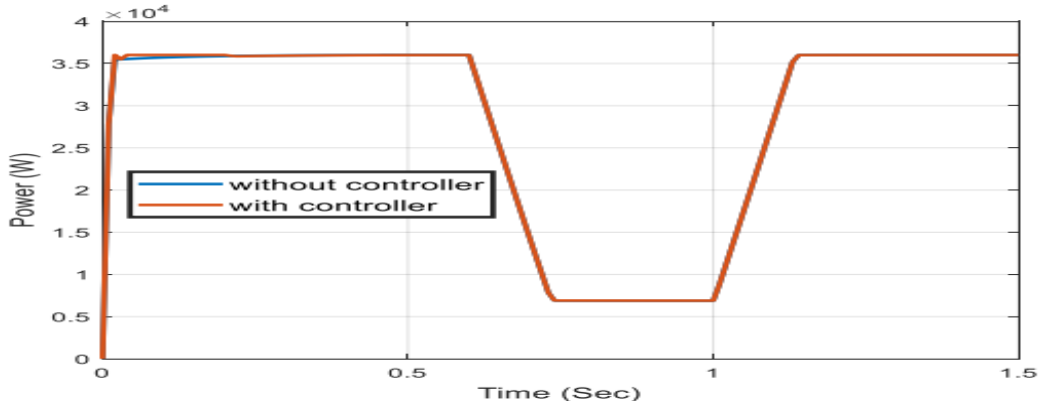

Figure 8: PV array output power for FLC MPPT controller

In all scenarios of irradiation, the simulation using the FLC controller reveals that the PV array power response produced from the PV array nearly matches the theoretically estimated results. According to the simulation results, the suggested FLC approach outperforms the directly linked system in all scenarios of rapid change in irradiation. As a result, the suggested FLC MPPT approach gains more daily pumped water than a directly linked system.

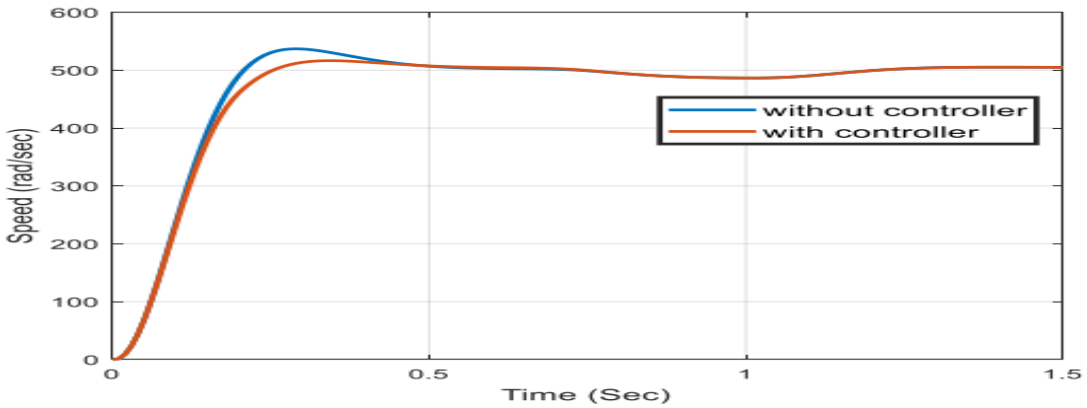

Figure 9: Rotational speed of motor for FLC MPPT controller

The performance index reveals that the FLC controller increases the rise time while decreasing the overshoot in the transient state. The oscillation is also eliminated using the fuzzy logic controller. The speed is inversely proportional to the flux and directly proportional to the voltage drop across the armature. As the armature voltage increases, so does the speed, and hence the flow rate or discharging rate.

Table 3: Performance characteristics of rotational speed of motor

Performance index	Without controller(directly)	With controller (FLC)
Rise time	131.563msec	149.068msec
Overshoot	6.989%, $t_p = 0.29sec$	2.577%, $t_p = 0.343sec$

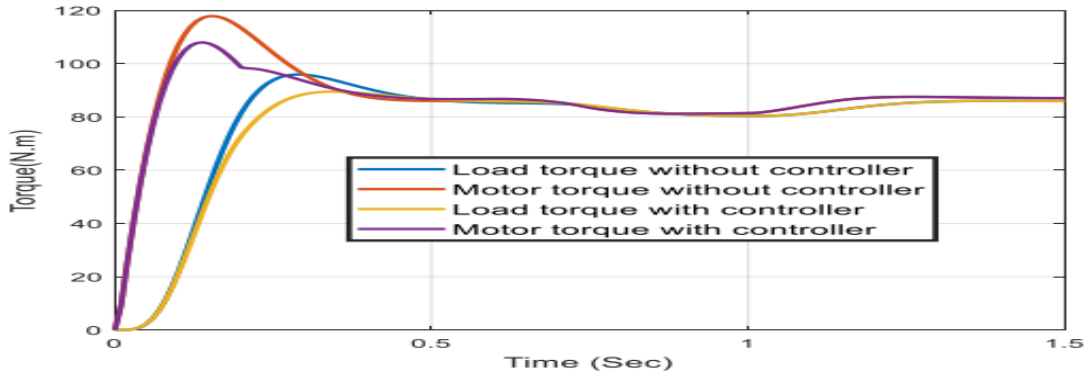

Figure 10: The load torque and motor torque MPPT controller

Table 4: Performance characteristics of motor torque and load torque

Performance index	Without controller(directly)	With controller(FLC)
Rise time of load torque	115.318msec	143.328msec
Rise time of motor torque	50.291msec	52.009msec
Overshoot of load torque	11.798%, t_p = 0.29sec	3.646%, t_p = 0.343sec
Overshoot of motor torque	36.3%, t_p = 0.153sec	24.375%, t_p = 0.137sec

The results of the performance measure demonstrates that in the transient state, the load and motor torque performance characteristics increase with rise time, while overshoot decreases. As a result, the overshoot eliminates the need for the FLC controller. The torque of an electric motor is proportional to the product of magnetic flux and armature current. Mechanical torque, also known as load torque, is proportional to the force-distance product. As a result, motor current varies with the amount of load torque supplied.

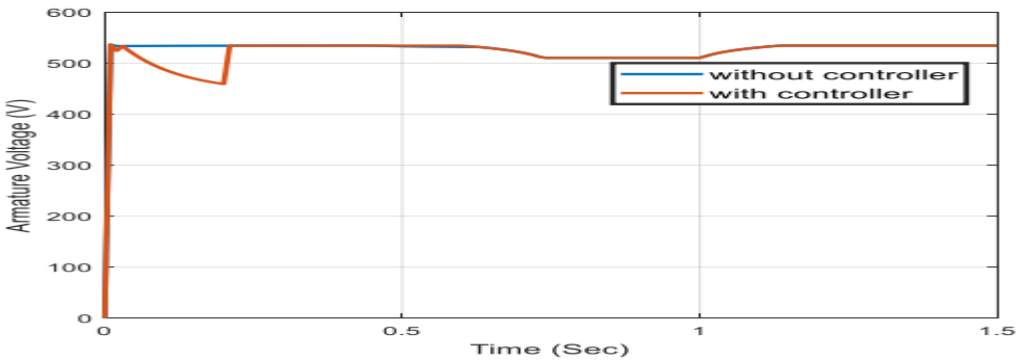

Figure 11: The armature voltage of motor MPPT controller

The simulation reveals that the armature voltage in the preceding figure, with and without the controller, is an overshoot in the directly linked system. The FLC control mechanism, on the other hand, eliminates overshoot. The armature voltage grows while the field current remains constant, and the speed also increases as the armature voltage increases. Increasing the speed means increasing the pumping rate.

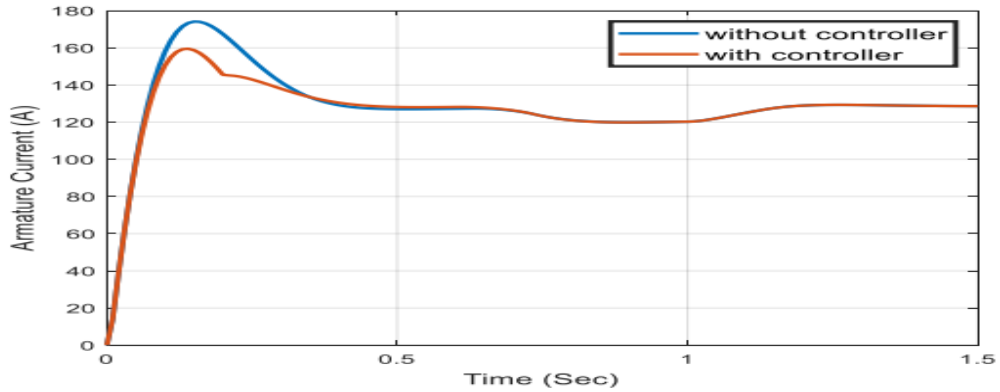

Figure 12: The armature current of motor MPPT controller

Table 5: Performance characteristics of armature current

Performance index	Without controller(directly)	With controller(FLC)
Rise time	50.291msec	52.009msec
Overshoot	36.3%, t_p = 0.153sec	24.375%, t_p = 0.137sec

According to the performance index, in a transient condition with an FLC controller, the rise time increases while the overshoot reduces. The oscillation is also eliminated using the fuzzy logic controller. When the armature current is increased, the speed reaches its maximum, and as a result, the charging rate or pumping rate increases.

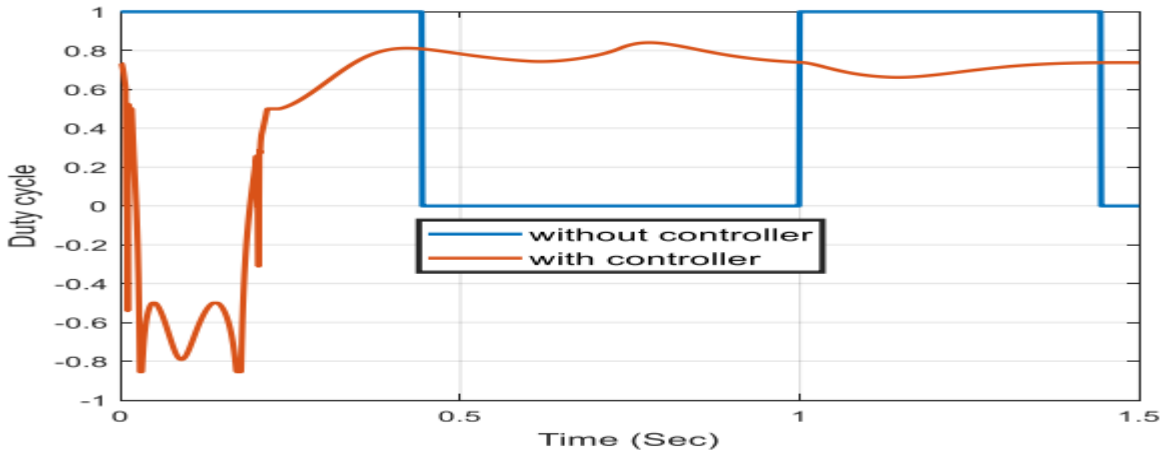

Figure 13: Duty ratio wave form of FLC with MPPT controller

The FLC's output signal (duty ratio) shifts to track the shifting optimum operating power point induced by irradiation fluctuations. PV array current, voltage, and power clearly fluctuate with solar irradiation in both systems, whether employing FLC or directly connected alternatives. The system with FLC, on the other hand, adjusts the duty ratio of the buck chopper to follow the updated MPP of the PV array. For roughly three seconds, the duty cycle with FLC exhibits a tiny wave. However, the controller changes the duty cycle with a little variation without going completely off.

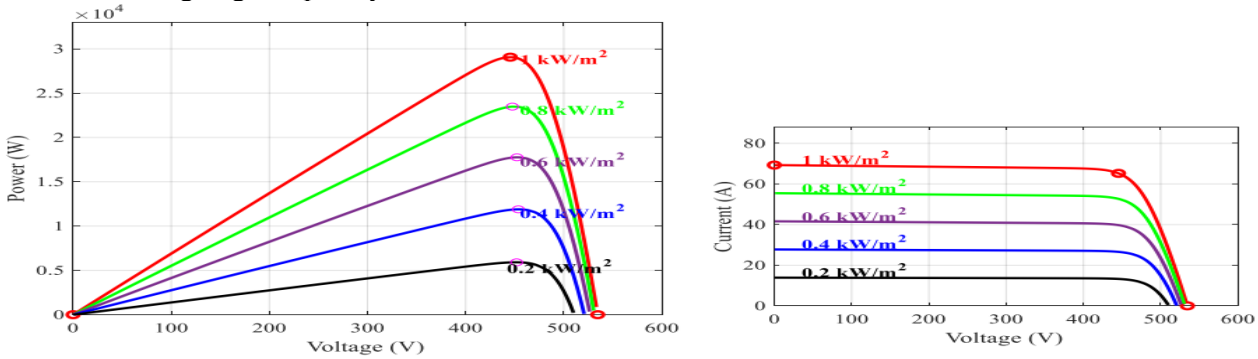

Figure 14: Operating points of PV system with MPPT controller on the P-V and I-V curves

The change in irradiance has a clear effect on the maximum PV output power at a constant temperature. It is evident that as the irradiation level rises, so will the PV output voltage and current. When the cell temperature remains constant, an increase in irradiation level corresponds to a theoretical increase in maximum power voltage. The short circuit current ISC, on the other hand, is completely and linearly dependent on the irradiance level.

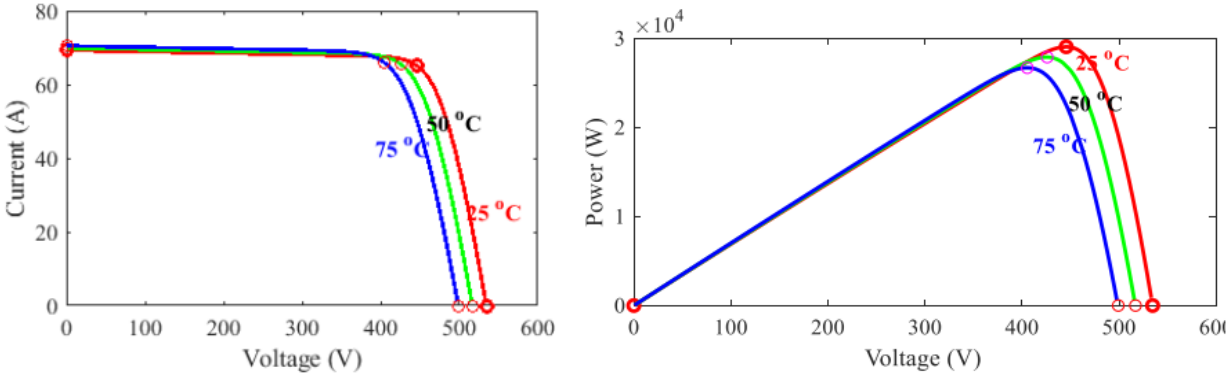

Figure 15: Operating points of PV system with MPPT controller on the P-V and I-V curves

Because of its effect on the output power of a solar panel, panel temperature is regarded as one of the most critical characteristics. The increase in panel temperature has a significant impact on the open circuit voltage. With a constant irradiation intensity, increasing the temperature leads in a modest increase in short circuit current because the band gap energy drops and more photons have enough energy to form electron-hole airs. The increases in temperature, on the other hand, have an apparent reduction in the PV panel output power due to the drop in the open circuit and the fill factor; hence, the module efficiency is reduced.
The direct system once connected with the best or the desired output signal at the MPPT which is ($D_{mppt} = 0.444$) and vary the environmental condition and compared with FLC controller.

Table 6: Performance comparison between FLC and Directly connected system

Irradiation	G(W/m2)	1000	400	200	1000	400	200	1000	400	200
Temperature	T (°C)	25	25	25	20	20	20	75	75	75
DIRECT	Calculated duty cycle(D)	0.849	0.844	0.724	0.803	0.806	0.724	0.851	0.823	0.820
	Output duty cycle Signal	0.444	0.444	0.444	0.444	0.444	0.444	0.444	0.444	0.444
	Error	0.405	0.4	0.28	0.359	0.362	0.28	0.459	0.853	0.376
	Efficiency(%)	91.12	90.09	63.06	80.08	81.53	63.06	91.66	85.36	84.66
	Total Efficiency (%)		81.17							
FLC	Calculated duty cycle(D)	0.850	0.851	0.844	0.845	0.843	0.833	0.887	0.856	0.835
	Output duty cyclesignal	0.444	0.444	0.444	0.444	0.444	0.444	0.444	0.444	0.444
	Error	0.406	0.405	0.4	0.401	0.399	0.1	0.43	0.412	0.391
	Efficiency(%)	91.44	91.21	90.09	90.31	90.31	87.61	99.77	92.79	88.06
	Total Efficiency (%)		92.17							
	Efficiency improvement by FLC		11							

4. Conclusion

A standalone solar water pumping system is provided in this study to provide water in isolated regions with a clean and sustainable source of electricity. The goal of this study was to increase total system efficiency by applying an effective MPPT technique to transmit the maximum available power to the load, especially when meteorological conditions changed. The FLC-based MPPT technique was demonstrated to have a relatively simple configuration consisting of two input variables and one output: the input variables are variations in PV array power and DC motor speed, and the output signal is the duty ratio for the buck chopper. Simulation is used to assess the performance of the fuzzy logic controller for the solar water pumping system. The simulation results reveal that the efficiency of the solar water pumping system with the fuzzy logic controller is 92.17%, whereas it is 81.17% without the controller. The simulation findings show that the suggested FLC technique outperforms the directly connected system in all circumstances of rapid changes in irradiation. As a result, the suggested FLC MPPT approach gains more daily pumped water than directly connected systems. Furthermore, the FLC system adjusts the duty ratio of the buck converter to monitor the PV's changed MPP.

5. Acknowledgments

First and foremost, I would like to thank God for enabling me to complete this work. I have taken efforts in this research which really would have been impossible without the indebted support and help of many individuals.

I would like to thank for school of electrical and computer Engineering (Industrial control Engineering chair for their friendly relation, giving advice and encouragement) likewise, I would like to thank for Ethio telecom for allowing me to study and for creating different learning opportunities from the beginning up to now.

6. Reference

Aashoor, F. A. O., & Robinson, F. V. P. (2012, September). A variable step size perturb and observe algorithm for photovoltaic maximum power point tracking. *2012 47th International Universities Power Engineering Conference (UPEC)*.

Anis, W. R., & Metwally, H. M. (1994, October). Dynamic performance of a directly coupled PV pumping system. *Solar Energy*, *53*(4), 369–377.

Barrett, J. D. (2007, November). Advanced Fuzzy Logic Technologies in Industrial Applications. *Technometrics*, *49*(4), 494–495.

Dadios, E. ed., 2012. Fuzzy logic: controls, concepts, theories and applications. BoD–Books on Demand.

Esram, T., & Chapman, P. L. (2007, June). Comparison of Photovoltaic Array Maximum Power Point Tracking Techniques. *IEEE Transactions on Energy Conversion*, *22*(2), 439–449.

Faranda, R., Hafezi, H., Leva, S., Mussetta, M., & Ogliari, E. (2015, May 26). The Optimum PV Plant for a Given Solar DC/AC Converter. *Energies*, *8*(6), 4853–4870.

Gonzalez-Llorente, J., Ortiz-Rivera, E. I., Salazar-Llinas, A., & Jimenez-Brea, E. (2010, February). Analyzing the optimal matching of dc motors to photovoltaic modules via dc-dc converters. *2010 Twenty-Fifth Annual IEEE Applied Power Electronics Conference and Exposition (APEC)*.

Illanes, R., De Francisco, A., Torres, J. L., De Blas, M., & Appelbaum, J. (2003). Comparative study by simulation of photovoltaic pumping systems with stationary and polar tracking arrays. *Progress in Photovoltaics: Research and Applications*, vol.11, pp.453-465.

Kashyap, M., Chanana, S., & Arya, J. S. (2013, April 1). *SOLAR POWERED PMDC MOTOR DRIVE | Atlantis Press*. SOLAR POWERED PMDC MOTOR DRIVE | Atlantis Press.

Kolhe, M., Kolhe, S., & Joshi, J. (2000, November). Determination of magnetic field constant of DC permanent magnet motor powered by photovoltaic for maximum mechanical energy output. *Renewable Energy*, vol.21, pp.563-571, 2000

Liu, X., & Lopes, L. (n.d.). An improved perturbation and observation maximum power point tracking algorithm for PV arrays. *2004 IEEE 35th Annual Power Electronics Specialists Conference,* PP.2005-2010.

Mohan, N., Robbins, W., Undeland, T., & Nilssen, R. (1994). Simulation of power electronic and motion control systems-an overview. *Proceedings of the IEEE*, *82*(8), 1287–1302.

Muta T. Hoshino M. Osakada, K. H., Hussein, K., Muta, I., Hoshino, T., & Osakada, M. (1995, January 1). *Maximum photovoltaic power tracking: an algorithm for rapidly changing atmospheric conditions*. '' Generation, Transmission and Distribution, IEE Proceedings-, vol.142, pp. 59-64, 1995.

N. Hajj Shehadeh, "solar-Driven water pumping: An untapped resource for Lebanon," CEDRO-UNDP, April 2015.

Ouoba, D., Fakkar, A., El Kouari, Y., Dkhichi, F., & Oukarfi, B. (April 2015). An improved maximum power point tracking method for a photovoltaic system. ICFPAM, Marrakech, Morocco.

UNEP, "water Policy and Strategy viewed on." www.unep.org/dpdl/water September 2015

Veerachary, M., Senjyu, T., & Uezato, K. (2002, July). Feedforward maximum power point tracking of PV systems using fuzzy controller. *IEEE Transactions on Aerospace and Electronic Systems*, *38*(3), 969–981.

Villalva, M., Gazoli, J., & Filho, E. (2009, May). Comprehensive Approach to Modeling and Simulation of Photovoltaic Arrays. *IEEE Transactions on Power Electronics*, *24*(5), 1198–1208.

Walker, G. (2001). Evaluating MPPT Converter Topologies Using a Matlab PV Model. Journal of Electrical & Electronics Engineering, Australia, 21(1), 49–55.

Yuvarajan, S., & Shanguang Xu. (n.d.). Photo-voltaic power converter with a simple maximum-power-point-tracker. *Proceedings of the 2003 International Symposium on Circuits and Systems, 2003. ISCAS '03.* pp.III, 399-402.